Methyl Halide Photochemistry on Iodine-Covered Pt(111)

Sam K. Jo† and J. M. White*

Contribution from the Department of Chemistry and Center for Materials Chemistry, The University of Texas at Austin, Austin, Texas 78712-1167

Received September 16, 1992. Revised Manuscript Received March 19, 1993

Abstract: The photon-driven dissociation of carbon–halogen bonds in methyl halides adsorbed on iodine-covered Pt(111) has been examined as a function of iodine coverage and of wavelength. For wavelengths which are not absorbed by gas-phase molecules, the photodissociation yield of monolayer amounts of adsorbed methyl halides *decreases* with increasing iodine coverage. For those wavelengths strongly absorbed in the gas phase, the photodissociation yield of the adsorbed phase *increases* with iodine coverage. These variations are analyzed using two model reaction paths, direct photon absorption and substrate-mediated electron attachment, exciting the methyl halide. We present evidence that, even when both paths are operative, a rising yield with increasing iodine atom coverage marks the dominance of direct photon absorption. From the phenomenological equations describing the latter reaction path, we conclude that the probability of electron attachment decreases more rapidly with iodine coverage than the probability of metal quenching.

Introduction

Both scientific and technological interests have motivated intensive study of the surface photochemistry of adsorbates,[1,2] resulting in some understanding of the roles played by the substrate.[3,4] Photon excitation can occur in at least two ways: first, analogous to homogeneous gas and liquid phases, by *direct adsorbate absorption* and, second, requiring the substrate, through *substrate absorption* followed by energy and/or charge transfer to the adsorbate. The relative importance of these two paths will depend, among other things, on the wavelength and on the adsorbate–substrate coupling in both the ground and excited states. Coupling strengths directly impact the excited-state-quenching probability and, thereby, the chemical events that occur. A desire to probe the relative importance of the direct and indirect excitation paths as functions of wavelength and adsorbate–substrate coupling motivated this work.

Methyl halides and iodine-covered Pt(111) were used to investigate these properties. Methyl halides (R–X) have been widely used as adsorbates for photon-driven studies for several reasons: (1) their surface structures and electronic properties are reasonably well-known; (2) except for iodides, they do not dissociate thermally on many metal and semiconductor surfaces (e.g., Pt(111), Ag(111), brominated Ni(111), and GaAs(110)); and (3) readily available ultraviolet (UV) photons from arc lamps and excimer lasers drive C–X bond cleavage.[5-9] Regarding Pt(111), the substrate used here, much is already known: (1) CH_3X adsorbs molecularly at ≤100 K with the halogen end bonded to the surface;[5,10] (2) upon heating, CH_3Cl and CH_3Br desorb molecularly, but a fraction of CH_3I dissociates into CH_3 and I, which lead to the desorption of CH_4 and I at higher temperatures;[5,10,11] (3) all three halides undergo C–X bond cleavage upon UV (λ = 250–300 nm) irradiation;[12-14] (4) threshold photon energies follow the gas-phase order $CH_3I < CH_3Br < CH_3Cl$, but photodissociation is red-shifted, compared with gas-phase data;[10,11] and (5) the photolysis rates (λ = 250–300 nm) of CH_3Cl[11] and CH_3Br[15-17] decrease sharply in passing from submonolayer to multilayer coverages, whereas for CH_3I[15] the opposite occurs.

Adsorbed iodine was used to decouple CH_3X and Pt. Several properties of predosed atomic iodine are known: (1) all coverages are thermally stable up to at least 500 K; (2) photoelectron emission is suppressed because the work function increases; and (3) the adsorbate–substrate interaction is weakened so that the first monolayer of CH_3X behaves in thermal desorption like a multilayer.[18]

By varying the photon energy distribution from a Hg arc lamp (using cutoff filters ranging from 5.3 to 3.6 eV) and the iodine coverage (from 0 to 0.43 ML), while keeping a fixed coverage of CH_3X (1 ML), we provide evidence for the varying roles played by substrate-mediated hot electron photochemistry and direct photon excitation of the adsorbate. Under some conditions, we can also set a lower bound on the extent of substrate quenching.

Experimental Section

A detailed description of the system has been given elsewhere.[11,19] Briefly, we used a turbo-pumped ultrahigh-vacuum (UHV) (2.5×10^{-10} Torr) system equipped for X-ray photoelectron spectroscopy (XPS), ultraviolet photoelectron spectroscopy (UPS), quadrupole mass spec-

† Current address: Coordinated Science Laboratory, University of Illinois, Urbana, IL 61801.

(1) (a) Chuang, T. *J. Surf. Sci. Rep.* **1985**, *158*, 525. (b) Ho, W. *Comments Condens. Mater. Phys.* **1988**, *13*, 293. (c) Polanyi, J. C.; Rieley, H. *Dynamics of Gas-Surface Interactions*; Rettner, C. T., Ashford, M. N. R., Eds.; Royal Society of Chemistry: London, 1990. (d) Richter, L. J.; Cavanagh, R. R. *Prog. Surf. Sci.* **1992**, *39*, 155.

(2) (a) Ibbs, K. G.; Osgood, R. M. *Laser Chemical Processing for Microelectronics*; Cambridge University Press: Cambridge, U.K., 1989. (b) Ehrlich, D. J.; Tsao, J. Y. *Laser Microfabrication—Thin Film Processing and Lithography*; Academic Press: New York, 1989.

(3) White, J. M. *Proc. SPIE-Int. Soc. Opt. Eng.* **1989**, *1056*, 129.

(4) Zhou, X.-L.; Zhu, X.-Y.; White, J. M. *Surf. Sci. Rep.* **1991**, *13*, 73.

(5) Henderson, M. A.; Mitchell, G. E.; White, J. M. *Surf. Sci.* **1984**, *184*, L325.

(6) (a) Zhou, X.-L.; Solymosi, F.; Blass, P. M.; Cannon, K. C.; White, J. M. *Surf. Sci.* **1989**, *219*, 294. (b) Zhou, X.-L.; White, J. M. *Surf. Sci.* **1991**, *241*, 244, 259, 270.

(7) Cho, C.-C.; Polanyi, J. C.; Stanners, C. D. *J. Phys. Chem.* **1989**, *92*, 6859.

(8) Marsh, E. P.; Gilton, T. L.; Meier, W.; Schneider, M. R.; Cowin, J. P. *Phys. Rev. Lett.* **1988**, *61*, 2725.

(9) Marsh, E. P.; Tabares, F. L.; Schneider, M. R.; Gilton, T. L.; Meider, W.; Cowin, J. P. *J. Chem. Phys.* **1990**, *92*, 2004.

(10) Roop, B.; Lloyd, K. G.; Costello, S. A.; Campion, A.; White, J. M. *J. Chem. Phys.* **1989**, *91*, 5103.

(11) Jo, S. K.; Zhu, X.-Y.; Lennon, D.; White, J. M. *Surf. Sci.* **1991**, *241*, 231.

(12) Costello, S. A.; Roop, B.; Liu, Z.-M.; White, J. M. *J. Phys. Chem.* **1988**, *91*, 1019.

(13) Zhou, Y.; Feng, W. M.; Henderson, M. A.; Roop, B.; White, J. M. *J. Am. Chem. Soc.* **1988**, *110*, 4447.

(14) Liu, Z.-M.; Costello, S. A.; Roop, B.; Coon, S. R.; Akhter, S.; White, J. M. *J. Phys. Chem.* **1989**, *93*, 7681.

(15) Liu, Z.-M.; Akhter, S.; Roop, B.; White, J. M. *J. Am. Chem. Soc.* **1988**, *110*, 8708.

(16) Jo, S. K.; White, J. M. Unpublished results.

(17) Zhou, X.-L.; White, J. M. *Chem. Phys. Lett.* **1990**, *167*, 205.

(18) (a) Jo, S. K.; White, J. M. *Surf. Sci.* **1992**, *261*, 111. (b) Jo, S. K.; White, J. M. *Surf. Sci.* **1991**, *255*, 321.

(19) Jo, S. K. Ph.D. Thesis, The University of Texas at Austin, 1990.

0002-7863/93/1515-6934$04.00/0

Table I. Desorption Peak Temperatures (K) of CH_3X on Pt(111)

	clean surface[a]		I-satd surface	
	1st layer	2nd layer	1st layer	2nd layer
CH_3I	240	133	150	137
CH_3Br	163	120	122	120
CH_3Cl	140	110	110 (127)	110

[a] CH_3X TPD spectra on I-free Pt(111) have also been reported previously.[5,10,11]

trometry (QMS), and temperature-programmed desorption (TPD). The Pt(111) sample (1 cm in diameter, 1 mm thick) could be cooled to 50 K by a closed-cycle He cryostat and flashed to 1400 K by resistive heating. A 6 K/s ramp rate was used for the TPD spectra.

CH_3X (99.5%) was dosed using a retractable tubular (0.25-in. diameter) doser positioned ~2 mm from the sample. The molecular flux to the surface was controlled by adjusting the pressure (1–5 Torr), measured by a capacitance manometer, behind a 2-μm pinhole located in the doser tube.[19] Precoverages of atomic iodine were prepared by repeated cycles, either dosing CH_3I at 60 K and annealing to 500 K[18] or dosing CH_3I, irradiating with UV light,[19] and annealing to 500 K. Saturation of the first layer of atomic I corresponds to 0.43 ML (i.e., 0.43 I per surface Pt atom),[18] and we use absolute coverages of I throughout this paper. For the methyl halides, we use an operational definition based on measured TPD peak areas: one monolayer is defined as the TPD peak area corresponding to saturation of the chemisorbed first layer of methyl halide (with no atomic iodine). We do not know the number of halide molecules per surface Pt atom.

XPS was performed with a hemispherical electron energy analyzer (40-eV pass energy and 0.05-eV step size) and a 300-W Mg Kα source (1253.6 eV). Binding energy (BE) values were referenced to the Pt($4f_{7/2}$) BE of 70.9 eV. Work function changes ($\Delta\Phi$) were measured by monitoring the shift of the secondary electron onset of He I UPS.

Photolysis was accomplished with a 100-W high-pressure Hg arc lamp.[19] With the full arc, the cutoff wavelength is 235 nm (hereafter, "≥235 nm"). Two long-pass cutoff filters were used to vary the wavelength distribution: one has 10 and 90% transmission at 295 and 330 nm, respectively (hereafter, "≥295 nm"), and the other has 10 and 90% transmission at 345 and 370 nm, respectively (hereafter, "≥345 nm"). The total yield of photoelectrons was measured using the hemispherical analyzer.

The key measurement, fractional photodissociation of one monolayer of CH_3X, was made using postirradiation TPD for CH_3Cl and CH_3Br and, because of parent thermal decomposition during TPD, XPS for CH_3I. To minimize X-ray beam damage (dissociation of CH_3I), the XPS scan time was limited to 15 min. Reproducibly controlled doses to prepare monolayer coverages of CH_3X were established in the absence of I(a) and, as described above, are based on TPD spectra which show saturation of the chemisorbed layer but no multilayer peak.[15]

Results

Influence of I on TPD Spectra. Table I shows how atomic iodine influences the peak temperatures in TPD spectra for both first and second (and higher) layers of CH_3X. On the clean, no I(a), surface, the first layer is chemisorbed and oriented with the halogen atom toward the substrate[5,10] and the separation of peak temperatures for the first and second layers is relatively large. This separation disappears in the presence of one saturated layer of atomic iodine (0.43 ML); by TPD, the first and second layers of CH_3X are indistinguishable, except for those of CH_3I, where a 13 K difference remains. We conclude that atomic iodine significantly reduces the attractive interactions between CH_3X and the substrate so that, in the presence of atomic I, the first CH_3X layer is almost indistinguishable from multilayers of CH_3X (see below).

CH_3I Photochemistry. Figure 1 shows postirradiation I($3d_{5/2}$) XP spectra of one monolayer of CH_3I on Pt(111) precovered with increasing amounts of atomic iodine (A→D). The same irradiation time (35 min) and photon energy range (≥235 nm) were used for all four spectra, and the I($3d_{5/2}$) signal from the initial I(a) has been subtracted.[18] Thus, each spectrum in Figure 1 represents both the remaining undecomposed CH_3I and the

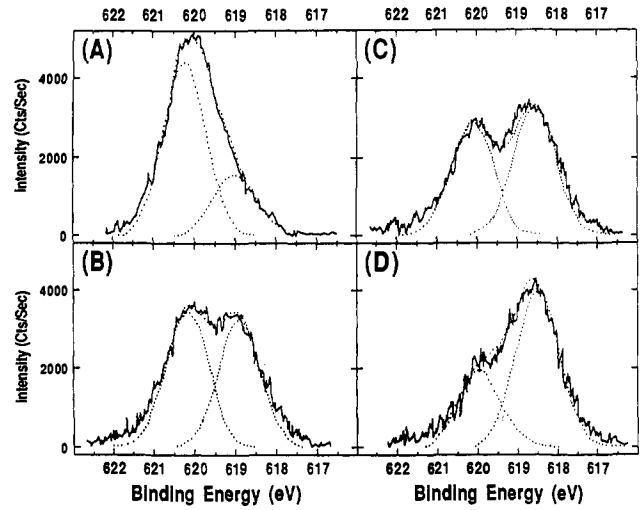

Figure 1. Postirradiation XPS of I($3d_{5/2}$) for 1 ML of CH_3I on (A) 0, (B) 0.10, (C) 0.17, and (D) 0.40 ML iodine-precovered Pt(111). Each spectrum is after 35 min of irradiation with full-arc (≥235 nm) Hg emission. The signal from the precovered iodine has been subtracted. Dotted curves represent curve fitting with two Gaussian peaks (between 620.4 and 619.9 and between 619.2 and 618.4 eV for CH_3I and I, respectively, with fwhm of 1.32 ± 0.01 eV).

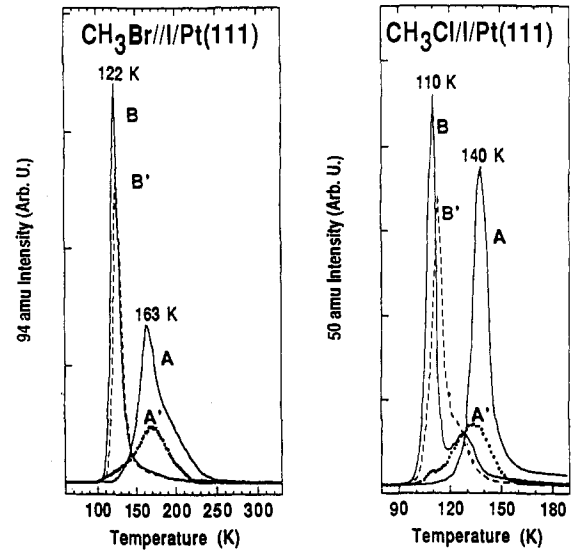

Figure 2. Left panel: TPD of 1 ML CH_3Br (94 amu) before (A and B) and after (A′ and B′) full-arc irradiation on clean (A and A′) and I-covered (B and B′) Pt(111). Right panel: TPD of 1 ML CH_2Cl (50 amu) before (A and B) and after (A′ and B′) full-arc irradiation on clean (A and A′) and I-covered (B and B′) Pt(111).

atomic iodine accumulated during photolysis. That the integrated areas of all four spectra are the same, within the experimental error, indicates the absence of photodesorption of either CH_3I or I. The dotted curves are synthetic Gaussian peaks with a fixed fwhm (1.32 eV) and previously determined BE's.[18] The fractional photolysis calculated as the ratio of the low (atomic I) BE peak area to the total XPS peak area clearly increases with the initial atomic iodine coverage.

CH_3Cl and CH_3Br Photochemistry. Since CH_3Br and CH_3Cl, unlike CH_3I, do not dissociate thermally on either clean or iodine-covered Pt(111), postirradiation TPD was used to determine their fractional photolysis. The photoinduced parent desorption is negligible,[11] so the measured decrease of the CH_3X TPD peak, after photolysis, corresponds to the fractional monolayer photodissociation. Figure 2 shows postirradiation TPD of one monolayer of CH_3Br (left panel) and one monolayer of CH_3Cl (right panel) on the clean and I-saturated (0.43 ML) surfaces. The strong CH_3X–substrate bonding interaction discussed above

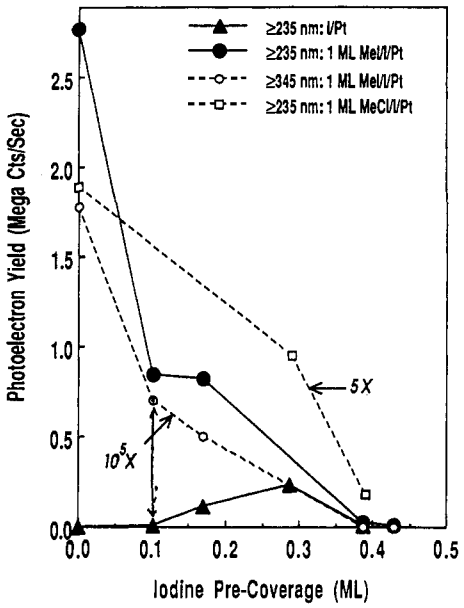

Figure 3. Photoelectron yield during UV irradiation from a Hg arc lamp with selected cutoff filters as a function of iodine percentage for various adsorbates and wavelength ranges. Note the multiplication factors (10^5 and 5).

(Table I) is weakened by adding I(a). Successful decoupling is indicated by the relatively sharp TPD spectra (B), the low desorption temperatures (multilayers desorb at 110 K (CH_3Cl) and 120 K (CH_3Br)[6,11]), and the nearly complete suppression of high-temperature desorption.

Photoelectron Yields and Fractional Photolysis. Photoelectron yields for various conditions are shown in Figure 3 (note large scaling factors) for various wavelength distributions. For $\lambda \geq 235$ nm, adding 0.17 ML of atomic I to Pt(111) (triangles) lowers the work function enough to allow photoemission, but the work function rises again, lowering the photoelectron yield, as the coverage approaches 0.43 ML.[18] Adding one monolayer of CH_3X to clean or I-covered surfaces always lowers the work function and increases the photoelectron yield, but the effect becomes smaller as the coverage of atomic I increases. Roughly speaking, for I(a) $\leq$ 0.25 ML, the yield of photoelectrons from CH_3I is 5-fold *higher* than that for CH_3Cl, but the difference decreases as I(a) approaches 0.43 ML. Comparing CH_3I at $\lambda \geq 235$ and $\lambda \geq 345$ nm, the photoelectron yields follow the same trends with increasing I(a), but the intensity is $\sim 10^5$ lower for the latter. The data for CH_3Br (not shown) show the same trends and lie between the results for CH_3I and CH_3Cl.

Of central importance, photolysis fractions as a function of the coverage of atomic iodine are plotted (Figure 4) for one monolayer of CH_3I (left panel) and of CH_3Br and CH_3Cl (right panel). For each curve, a different but fixed photolysis time was chosen to give reliably measurable photodissociation. In the absence of I(a) and with $\lambda \geq 235$ nm irradiation, the fractional photolysis was in the order $CH_3Br > CH_3Cl > CH_3I$; i.e., 50% of CH_3Br was dissociated in 12 min, 50% of CH_3Cl was dissociated in 35 min, but only 30% of CH_3I was dissociated in 35 min. This order differs from the C–X bond energies, which suggests that CH_3I would be easiest to photolyze. It also differs from the ordering of the photoelectron yields, $CH_3I > CH_3Br > CH_3Cl$. For I(a) = 0.25 ML, keeping $\lambda \geq 235$ nm, the fractional photolysis order changes to $CH_3I > CH_3Br > CH_3Cl$. Strikingly, while iodine precoverage (Figure 4) always *suppresses* the photochemistry of CH_3Br and CH_3Cl, it *enhances* CH_3I photolysis when $\lambda \geq 235$ nm and *suppresses* it for $\lambda \geq 345$ nm. The switch for CH_3I occurs even though the photoelectron yield follows the same *downward* trend with I(a) for both wavelength regimes.

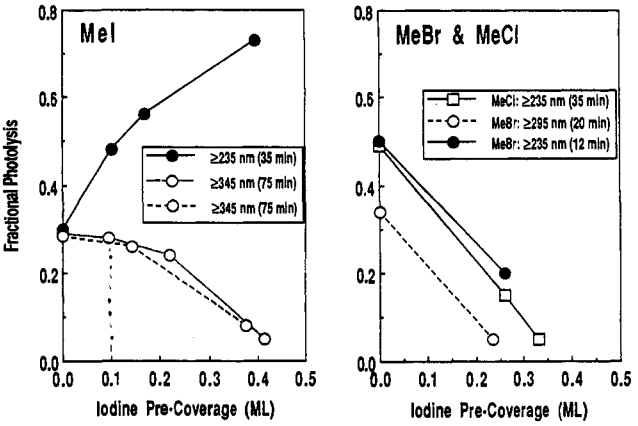

Figure 4. Fractional photolysis yield as a function of iodine coverage for 1 ML of CH_3I (left panel) and of CH_3Br and CH_3Cl (right panel). Wavelengths and irradiation times are indicated. The atomic iodine coverages were determined by normalizing the maximum XPS area to the absolute (I/Pt atom number ratio) saturation coverage of 0.43 as detailed previously.[18]

Discussion

Before discussing these very interesting wavelength and iodine coverage dependences, we note several known photochemical properties relevant in the absence of atomic I.[10,11] Photon-driven C–X bond cleavage occurs with different threshold photon energies (see Table II). For $\lambda \geq 235$ nm, all three halides are photolyzed; for $\lambda \geq 295$ nm, CH_3Cl is not photolyzed; and for $\lambda \geq 345$ nm, neither CH_3Cl nor CH_3Br is photolyzed. Further, consistent with what we report here, previous work[10,11] shows that photon-driven parent desorption is negligible, that large fractions of the CH_3 fragments, and all the halogens, are retained on the surface, and that the postirradiation TPD products are CH_4, H_2, HX, and/or X. We now discuss the effects of iodine coverage and wavelength regime.

Model. We describe all the results in terms of a model, outlined in the Introduction, involving two excitation channels for photon-driven CH_3X dissociation—substrate-mediated hot electron attachment and direct adsorbate excitation.[4,7,8] In the former, the substrate plays a key role by absorbing photons and producing excited electrons which activate CH_3X by attachment to form a temporary anion. In the latter, photons are absorbed directly by CH_3X with a wavelength dependence characteristic of the molecule. Typically, for CH_3X, the substrate-mediated process has an adsorbate-dependent threshold at wavelengths longer than the threshold wavelength for direct absorption (Table II). The two paths can become competitive for photon energies well above the threshold, i.e., where the direct excitation probability becomes comparable with the electron attachment probability. While the excited CH_3X states differ (one is anionic, the other neutral), both are dissociative with respect to the C–X bond and both, when in direct contact with a metal substrate, can be quenched on a subpicosecond time scale. In the subpicosecond time interval after excitation and before quenching, the repulsive character of the excited-state potential energy along the C–X direction leads to elongation and accumulation of momentum in that coordinate. Sufficient elongation/accumulation can activate the adsorbate for C–X cleavage either before or after quenching. After quenching, the required activation energy can be retained in the ground-state adsorbate, e.g., as vibrational excitation. While this vibrational excitation would not be sufficient in the gas phase, the presence of chemically active Pt atoms can make the barrier sufficiently low to allow C–X cleavage.

We can cast the description in terms of chemical reaction steps for the two possible excitation paths. For the substrate-mediated path, with overall cross section σ_1

Table II. Photodissociation (C–X Bond Cleavage) of CH_3X on Clean Pt(111)[10,11]

	≥235 nm ≥5.3 eV	≥295 nm ≤4.2 eV	≥345 nm ≤3.6 eV	Φ,[a] eV	λ_{max},[b] nm (eV)	$\sigma \leq 10^{-22}$ cm^2 [c] nm (eV)
CH_3Cl	yes[d]	no	no	4.55	170 (7.30)	220 (5.64)
CH_3Br	yes	yes	no	4.20	200 (6.21)	280 (4.43)
CH_3I	yes	yes	yes	3.55	260 (4.78)	350 (3.55)

[a] The work function (±0.05) of 1 ML CH_3X-covered Pt(111) determined in this work. [b] Gas-phase UV absorption exhibits a smooth curve for all three halides with maximum absorptions at λ_{max};[27] the absorption cross sections at λ_{max} are $\sim 10^{-18}$ cm^2/molecule.[20] [c] Photon wavelength or energy for which the gas-phase C–X bond dissociation cross section would fall below our detection limit.[20,26] [d] "Yes" means successful C–X bond cleavage.

$$CH_3X(a) + I/Pt(111) + h\nu \rightarrow CH_3X(a) + I/Pt(111) + e^- \quad \sigma_e \quad (1)$$

$$e^- + CH_3X(a) \rightarrow CH_3X(a)^- \quad P_a \quad (2)$$

$$CH_3X(a)^- \rightarrow X(a)^- + CH_3(a \text{ or } g) \quad P_e \quad (3)$$

where step 1 assumes a photon is absorbed in the metal and, with cross section σ_e, excites an electron, step 2 represents a complex series of subsequent steps including transport to and tunneling through any barriers at the surface and electron attachment to CH_3X, and step 3 represents dissociation of the C–X bond. P_i denotes the conditional probability of step i and σ_j is the cross section for process j. As defined here, step 1 makes no distinction between energetic electrons above and below the vacuum level. The excitation cross section, σ_e, varies, at most, weakly as atomic iodine is added because the optical properties of the system change very little. Both the electron potential energy barrier (between the Pt substrate and the CH_3X adsorbate) and the energy separation between the Fermi level and the electron affinity level of CH_3X increase rapidly with iodine coverage. These factors must be contained in P_a. They also influence P_e, but the latter also involves variations with iodine coverage of the repulsive potential that leads to activation of the C–X bond.

Similarly, for the direct dissociation path, with overall cross section σ_2

$$CH_3X(a) + I/Pt(111) + h\nu \rightarrow CH_3X(a)^* + I/Pt(111) \quad \sigma_p \quad (4)$$

$$CH_3X(a)^* \rightarrow X(a) + CH_3(a \text{ or } g) \quad P_p \quad (5)$$

where step 4 denotes the absorption of a photon by the adsorbed halide and step 5 the bond dissociation.

In terms of these two paths, the overall cross section can be written as the sum

$$\sigma = \sigma_1 + \sigma_2$$

$$\sigma = \sigma_e P_a P_e + \sigma_p P_p$$

$$\sigma = \sigma_e P_a (1 - Q_e) + \sigma_p (1 - Q_p)$$

where Q_i is the quenching probability for all excited states, including vibrationally excited electronic ground states, formed in process i.

For direct absorption, we assume that σ_p tracks the known gas-phase absorption cross section, independent of the conditions at the surface; i.e., σ_p will remain constant as the coverage of I(a) changes but will rise as the photon energies increase. Quenching, which we expect to be highest for molecules directly coupled to the surface, will make σ_2 smaller than σ_p. As I(a) is added, we expect quenching to decrease and the dissociation cross section, σ_2, to rise.

For substrate-mediated excitation, σ_1, we expect the substrate excitation cross section, σ_e, to be independent of I(a) but to increase slowly with photon energy. For a given photon regime, we expect that adding I(a) will alter both the number of hot electrons within the resonant electron attachment energy range[4,8,9] and the electronic coupling that occurs at the substrate surface. Both factors contribute to P_a. Quenching, Q_e, from anionic states will differ from that for directly excited states, Q_p; their coupling to the surface is qualitatively different due to charge-image charge stabilization in the former. At its simplest, adding atomic I makes no change in σ_e, reduces adsorbate–substrate coupling to drive P_a down, and reduces quenching, making $(1 - Q_e)$ larger. The net effect on σ_1 will depend on how the falling P_a compares with the rising P_e as I(a) increases.

Considering the two paths together, we would interpret a measured decrease of the bond dissociation yield with increasing I(a) coverage as definitely indicating that substrate-mediated excitation dominates. An increased bond dissociation yield is not as easily interpreted, but as outlined below, we favor the direct excitation path.

Interpretation of Data. Within this model framework, we now consider the data. With the exception of CH_3I and $\lambda \geq 235$ nm (Figure 4 and Table II), which must be considered separately, substrate-mediated excitation clearly dominates for every wavelength regime and every methyl halide. First, consider CH_3Br. For $235 < \lambda < 300$ nm, gas-phase CH_3Br absorbs light, albeit weakly and dissociates.[20] For CH_3Br adsorbed on brominated Ni(111), there is evidence for a significant contribution of direct excitation, e.g., CH_3 fragment time-of-flight data, and of substrate-mediated excitation.[9] However, as shown in Figure 4, the photolysis yield *decreases* as atomic I is added, and we conclude that, for our conditions, the substrate-mediated channel dominates. Turning to CH_3Cl, gas-phase absorption for $\lambda \geq 235$ nm is negligible, so substrate-mediated excitation is expected, consistent with our observations.

The CH_3I case is most interesting because, as the wavelength regime passes from ≥235 to ≥345 nm, there is a marked reversal of the effect of adding atomic iodine—from yield enhancement to inhibition. On the basis of the above analysis, we conclude that substrate-mediated excited dominates for $\lambda \geq 345$ nm. This is expected since gas-phase absorption by CH_3I in this regime is even weaker than that by CH_3Br in the regime $\lambda \geq 235$ nm.

The rise of the dissociation yield with I(a) for CH_3I(a) and $\lambda \geq 235$ nm requires further consideration. In terms of the above model, dominant direct excitation ($CH_3I(a) + h\nu \rightarrow [CH_3I]^* \rightarrow CH_3$(a and g) + I(a)) is the simplest explanation. A switch from dominance by substrate mediation to direct absorption is not surprising considering the gas-phase data (Table II);[3] i.e., the photon absorption cross section increases by more than 4 orders of magnitude between 345 and 235 nm. The only way for a substrate-mediated process to dominate is for the product $P_a(1 - Q_e)$ to increase with I(a) coverage. But since this product decreases with increasing I(a) for every other case reported here, particularly for CH_3I and $\lambda \geq 345$ nm, it is difficult to find a compelling reason for the opposite effect at shorter wavelengths. For all monolayer coverages of methyl halides (Figure 3), the yield of photoelectrons always drops as I(a) increases. While this only measures those electrons above the vacuum level, not

(20) Okabe, H. *Photochemistry of Small Molecules*; Wiley: New York 1988.

all the electrons excited above the Fermi level, it is difficult to imagine that the number of excited electrons meeting the resonant energy requirement for attachment increases with I(a) when $\lambda \geq 235$ nm but decreases when $\lambda \geq 345$ nm. Thus, we strongly favor direct excitation as dominating, with a smaller, but nonnegligible, substrate-mediated contribution at $\lambda \geq 235$ nm.

We now consider how substrate quenching will vary with I(a). Because I(a) reduces the coupling between the methyl halide and the substrate, we generally expect its addition to reduce quenching probabilities for either excitation path; i.e., both P_e and P_p will increase. But, for the substrate-mediated path, adding I(a) has an additional major effect; the attachment probability, P_a, drops because the number of low-energy electrons incident on the space occupied by CH_3X is greatly reduced. For those electrons above the vacuum level, this effect is evidenced by the results of Figure 3. For those electrons below the vacuum level, the situation is more complicated. The fraction of the excited electron distribution appearing below the vacuum level will increase with I(a), but the number of electrons incident on CH_3X is overwhelmingly lower because the effective electron potential barrier (height and width) increases with I(a).[3,4] Turning to the results of Figure 4, we interpret the low photolysis yield for $\lambda \geq 345$ nm, largely in terms of lower P_a, but with significant contributions from P_e.

The $\lambda \geq 235$ nm CH_3I photolysis curve (Figure 4) suggests that an asymptotic dissociation yield will be realized at I coverages above 0.43 ML of I. On the basis of all the photoelectron yield data and the loss of photodissociation activity in all the other cases, we interpret the 0.75 fractional photolysis of CH_3I at 0.42 ML of I(a) as almost entirely due to direct excitation. Quenching, by the metal, still plays a role since the photodissociation yield has not reached its asymptotic value.

Charge Transfer. We now examine the role of charge transfer in more detail. In the absence of I(a), CH_3Cl photolysis by electron attachment requires excited electrons above the vacuum level.[4] But CH_3Br and CH_3I photolysis occurs even when no photoelectrons are produced; energetic electrons below the vacuum level by no more than 0.6 eV will drive dissociation (Table II). Assuming that gas-phase electron attachment processes are analogous, this energy requirement is reasonable since dissociative electron attachment (DEA) to $CH_3X(g)$ occurs resonantly with maximum cross sections at very low (<0.5 eV with respect to vacuum) electron kinetic energies in the order $CH_3I < CH_3Br < CH_3Cl$[21-23] and since stabilization of anionic adsorbed states by image-charge forces is expected.

The adsorbate electron affinity (EA) levels are expected to fall in the order $CH_3I(a) < CH_3Br(a) < CH_3Cl(a)$ (the EA's are +0.25–0.35, –0.46, and –3.45 eV for gas-phase CH_3I, CH_3Br, and CH_3Cl, respectively.[24] Moreover, the potential barrier for electron transfer between Pt and CH_3X is expected to be lowest for CH_3I followed by CH_3Br and CH_3Cl. Thus, the hot electron contribution to the photolysis is expected to increase in the order $CH_3Cl < CH_3Br < CH_3I$. Considering their respective work function (Table II) and photoelectron yield data (Figure 3), the ≥295-nm CH_3Br photolysis and ≥345-nm CH_3I photolysis must be dominated by the tunneling attachment of hot electrons, while photoelectrons dominate the CH_3Cl photolysis.[11] The suppression of substrate-mediated dissociation as I(a) increases is consistent with the DEA mechanism;[8,9,11] i.e., fewer electrons with resonant energies reach the adsorbate.

In the case of ≥235-nm CH_3I photolysis, which we have intrepreted in terms of direct photon excitation, substrate quenching should manifest itself as an increased fractional photolysis as I(a) is added. From the increased fractional photolysis, 0.3 to 0.7 for ≥235 nm in Figure 4 due to increased I(a), we conclude that more than 50% of the directly excited CH_3I molecules not only are quenched but also do not dissociate. Under conditions where the effect of I(a) is the opposite, e.g., $\lambda \geq 345$ nm, the monotonically decreasing CH_3I photolysis yield with increasing iodine precoverage (Figure 4) can be understood by the overwhelming effect of the decreasing number of effective electrons (due to the higher work function. Though substrate quenching in the DEA-dominated instances is not so self-evident as in the direct photon dissociation, we, in a separate work,[25] present evidence for the strong quenching (>90%) of ≥235-nm CH_3Cl photolysis.[11]

It is interesting that, for $\lambda \geq 235$ nm, fractional photolysis increases in the order $CH_3I < CH_3Cl < CH_3Br$ on the I-free surface. This suggests that CH_3I dissociation is much more strongly quenched than CH_3Br and CH_3Cl dissociation.[15] This was unexpected, even if there is complete quenching of direct photon dissociation, because compared to the cases for CH_3Cl and CH_3Br there are more excited electrons at all energies for the CH_3I-covered surface (Table II and Figure 3). Thus, we conclude that the metal quenching probability is highest, by far, for CH_3I. This may result from stronger coupling of I[15] with Pt. Further investigations with higher photon energies for CH_3Br (6.2 eV) and CH_3Cl (7.3 eV) will shed more light on this issue.

Conclusion

To summarize, we have determined the effects of wavelength and atomic iodine coverage on the probability of photon-driven C–X bond dissociation in methyl halides molecularly adsorbed on Pt(111). Kinetic models are discussed for dissociation initiated by substrate-mediated electron attachment and direct photon absorption processes. For one monolayer of methyl chloride, bromide, and iodide, adding atomic iodine decreases the dissociation yield for all ultraviolet wavelength regimes except one, $\lambda = 235$ to ~300 nm for CH_3I, where the yield rises rapidly as atomic iodine is added. This rise is consistent with direct photon absorption of CH_3I to a dissociative state and reduced quenching of this state with added atomic I. All the other cases are dominated by substrate-mediated excitation where the added I(a) reduces the cross section for electron attachment. By comparing the C–I dissociation yields at $\lambda \geq 235$ nm, with and without atomic iodine coverage, we estimate that at least 50% of directly excited CH_3I molecules are quenched in the absence of I(a). Pt quenching vanishes when the CH_3I lies more than two layers away from the metal. Interestingly, quenching by Pt of the transient anion, CH_3I^-, is higher than that for the other two halides. We attribute this to stronger coupling of the halogen to Pt.

Acknowledgment. This work was supported in part by NSF Grant CHE9015600.

(21) Petrovic, Z. Lj.; Wang, W. C.; Lee, C. J. *J. Chem. Phys.* **1989**, *90*, 3145.
(22) Massey, H. *Negative Ions*, 3rd ed.; Cambridge University Press: Cambridge, U.K., 1976.
(23) Stockdale, J. A.; Davis, F. A.; Compton, R. N.; Klots, C. E. *J. Chem. Phys.* **1974**, *60*, 4279.
(24) Christophorou, L. G. *Electron-Molecule Interactions and Their Applications*; Academic Press: New York, 1984.
(25) Jo, S. K.; Kiss, J.; Castro, M. E.; White, J. M. *ACS Symp. Ser.* **1992**, *482*, 310.
(26) Calvert, J. C.; Pitts, J. N. *Photochemistry*; Wiley: New York, 1966.
(27) Felps, W. S.; Rupnik, K.; McGlynn, S. P. *J. Phys. Chem.* **1991**, *95*, 639.